PLATE LOADING TESTS ON A GEOSYNTHETIC REINFORCED SHALLOW EMBANKMENT: FIELD MEASUREMENTS AND NUMERICAL MODELLING

R. Banjac, P. A. Mayor
Institute for Geotechnical Engineering, Swiss Federal Institute of Technology Zurich, Switzerland
R. Hufenus
Swiss Federal Laboratories for Materials Testing and Research, St. Gall, Switzerland

ABSTRACT: Plate compression tests were performed on a shallow road embankment reinforced with a single geosynthetic layer at different construction stages. The geosynthetic has been laid on the subgrade material and three layers have been placed and compacted by a vibrating roller. These construction processes and the subsequent plate loading test have been modelled with a FE-Program using an axisymmetric approach. Different constitutive models have been selected and a parameter study, using a range of soil properties, has been carried out. Additional considerations have been made over the interaction between the soil and the geosynthetic as well as the modelling of the stress-strain response of the geosynthetic. The results of the parametric study are presented in comparison with the results of the field tests

1 INTRODUCTION

Geosynthetics are often used under shallow embankments on soft ground to improve the compaction properties and the long-term bearing capacity and serviceability. The reinforcing layers are often designed using conventional geotechnical methods based on ultimate limit states. These methods allow the reinforcement to be designed but are not suitable for predicting the serviceability of the reinforced structures. The present paper is a part of the research project „Design of Geosynthetic Reinforcement", which aims to give guidelines for the design of serviceability and ultimate limit states.

Due to the complexity of these systems consisting of materials with totally different mechanical properties, geosynthetic reinforced structures are more and more modelled with the help of numerical methods. The difficulties in using this method consist, beside the use of appropriate soil parameters, in the appropriate choice of the constitutive laws for the soil and of the parameters for the soil-structure interaction. Therefore of the problem, the calculation method has to be validated with the help of laboratory and field tests.

In this study, field plate loading tests on a geosynthetic reinforced shallow embankment are back-calculated in order to assess the usability of the finite element method to predict the behaviour of such a reinforced structure.

2 FIELD TESTS

The plate loading tests, as part of an intensive field test programme (HUFENUS et al., 2003, 2004), were performed on a test track built within the framework of the research project mentioned above. The test site is located in a brick clay mining pit near Schaffhausen in Switzerland. The test track (Figure 1) had a length of about 130 m allowing the installation of ten different geosynthetics (five geogrids, one geocomposite, two nonwovens and two slit tape wovens (one deliberately weak)) as a reinforcement layer.

The sub-grade consisted of relatively homogenous clayey silt with a very low bearing capacity over the whole length of the track.

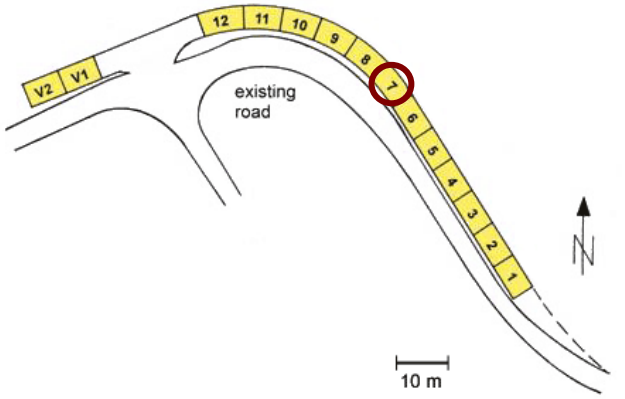

Figure 1 Test track with division between fourteen fields

Loose recycled material (crushed concrete) was used to build the embankment layers. The test track was built with three 0.2 m layers, the first layer being compacted statically, and the 2nd and 3rd dynamically (Figure 2). Static plate loading tests were performed on top of each layer.

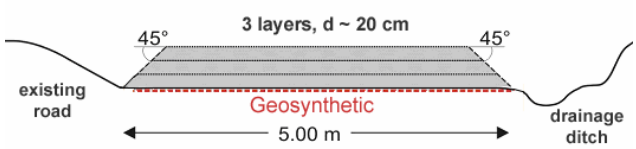

Figure 2 Cross section of the test track

In order to measure the short and long term strain, the geogrids have also been equipped with strain gauges (Figure 3). These gauges have been calibrated through tension tests in the laboratory and their resistance to damage during the construction process was tested before construction.

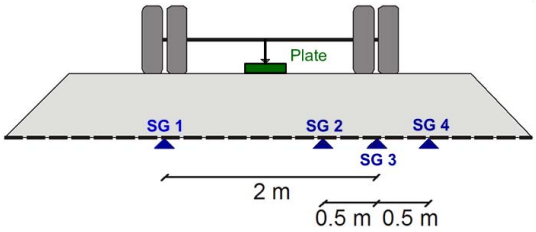

Figure 3 Cross section of the embankment, position of the strain gauges, field 7

In this paper, the results of the Finite Element calculations of plate loading tests on one of the fourteen fields (field 7) on the first and second embankment layers are presented and discussed.

3 MATERIAL PROPERTIES

3.1 *Soil Properties*

The subgrade consisted of relatively homogenous clayey silt, classified according to the Swiss code SN 670 008a as a middle plasticity clay (CM).

The subgrade was overconsolidated and has been loosened up before construction by an excavator. It was not possible to remove completely the effects of overconsolidation, so an overconsolidation ratio of 2 has been adopted for the numerical modelling.

The peak strength envelope was determined from two undrained triaxial tests and the deformability from an oedometer test:

Cohesion	$c' = 25$ kN/m^2
Friction angle	$\varphi' = 14°$
Dilation angle	$\psi' = 0°$
Compression index	$C_c = 0.249$
Swelling index	$C_s = 0.031$
Initial void ratio	$e_{ini} = 0.85$
Saturated unit weight	$\gamma_{sat} = 18.9$ kN/m^2
Permeability	$k = 2.89 \times 10^{-9}$ m/s

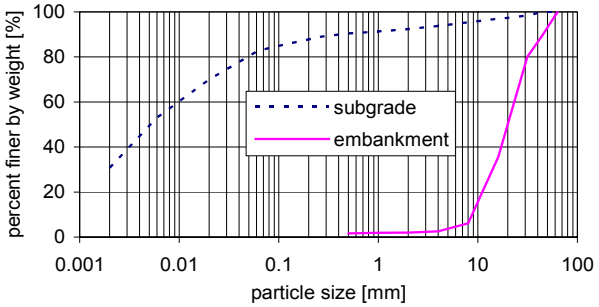

Figure 4 Particle size distribution of the subgrade and embankment layers

Loose recycled material consisting of crushed concrete was used for the construction of the embankment. The stiffness and the strength parameters were determined by parameter studies. In the literature (e.g. SCHANZ, 1995) a high shear resistance with a high dilatancy and also cohesion due to interlocking is given for such materials. In this paper, the following ranges of strength and stiffness for the embankment has been studied:

Cohesion	$c' = 5$ -15 kN/m^2
Friction angle	$\varphi' = 35°$ -45°
Dilation angle	$\psi' = 5°$ -15°
Stiffness	$E = 15$-25 MN/m^2

3.2 *Geosynthetic Properties*

The reinforcement consisted of an extruded biaxial Polypropylene (PP) grid (width = 3.80 m, grid 65 x 65 mm). Table 1 contains details about the mobilised strength of the product (manufacturer's data).

Table 1 Mobilized tensile strength of the products at different strain levels

Field 7	tensile strength machine/cross direction [kN/m]		
	at 2 %	at 5 %	max.
	11/12	22/25	30/30

It is well known that the tensile stiffness of the geogrids determined in traction tests is highly dependent upon the loading velocity. In order to obtain realistic values for the tensile stiffness, traction tests have been performed at a velocity v corresponding to the relatively low velocity of the plate loading test (v = 5 mm/min). The geogrid was also un- and reloaded in the same way as in the plate loading tests to determine the reload tensile strength (HUFENUS, 2003).

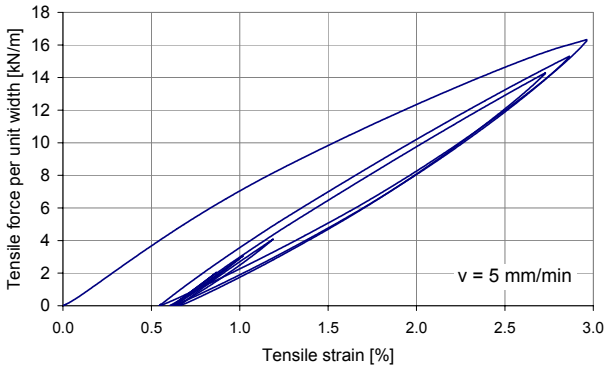

Figure 5 Tensile force-strain curve of the geogrid (HUFENUS 2003)

For both embankment layers, tensile secant moduli in terms of tensile force per unit width normalised by tensile strain have been calculated for the load and un-/reload phases. The maximum tensile strength for this geogrid was 30 kN/m.

Table 2 Tensile secant moduli of the geogrid

Tensile secant modulus [kN/m]	Loading	Un-/Reloading
1st Embankment Layer	550	700
2nd Embankment Layer	800	850

4 RESULTS OF THE FIELD TESTS

The plate loading tests were carried out on each embankment layer and each test field to measure the deformability and load-bearing capacity at the different stages of the construction. Using a one dial gauge plate loading device (∅ = 300 mm), the tests have been carried out in three stages (loading, unloading, reloading) with different loading steps as defined in the Swiss standards. Because the subgrade was so soft, it was not possible to reach the maximal load required by the standards, which corresponds to a load of 0.5 MN/m^2, in some fields.

Consolidation also took place during the test and made it impossible to expect a minimal settlement change per minute according to the standards (Swiss Norm <0.02mm/min). The results of the plate compression test were analysed according to the Swiss Norm SN 670 317b,

which gives a modulus of deformation E_V (= Young's moduli E). E_1 is the modulus for loading, E_2 the one for re-loading.

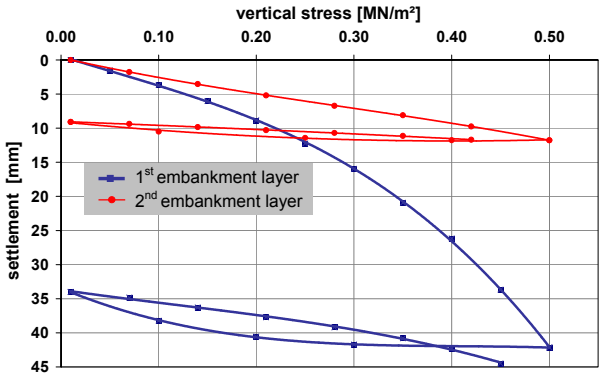

Figure 6 Load-settlement curves, plate loading test on 1st and 2nd embankment layer, field 7

Table 5 Measured Young's moduli E_1, E_2 on the 1st and 2nd layer, field 7

Young's moduli [MN/m²]	E_1	E_2	E_2/E_1
1st embankment layer	2.85	9.92	3.49
2nd embankment layer	9.84	35.55	3.61

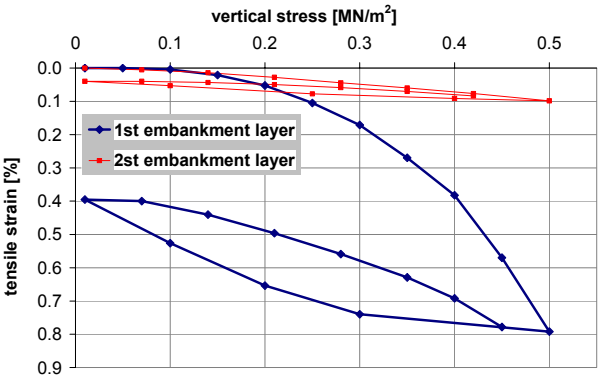

Figure 7 Measured strains (strain gauge 2), plate loading test on 1st and 2nd embankment layer, field 7

5 NUMERICAL MODELLING

The numerical modelling was carried out using the Finite Element Program PLAXIS V8.2 (BRINKGREVE 2002) assuming axi-symmetric conditions. An updated mesh analysis was performed to take into account the effect of the deformation especially that of the geogrid (tension stiffening effect).

5.1 *Boundary conditions*

A half-width of 2.25 m and a depth of 2.0 m were chosen for the mesh of the subgrade. Standard fixities (horizontal fixities on the vertical borders, total fixities on the bottom) have been applied (Figure 8).

The groundwater table was assumed to be at the surface of the subgrade, which was considered to be saturated.

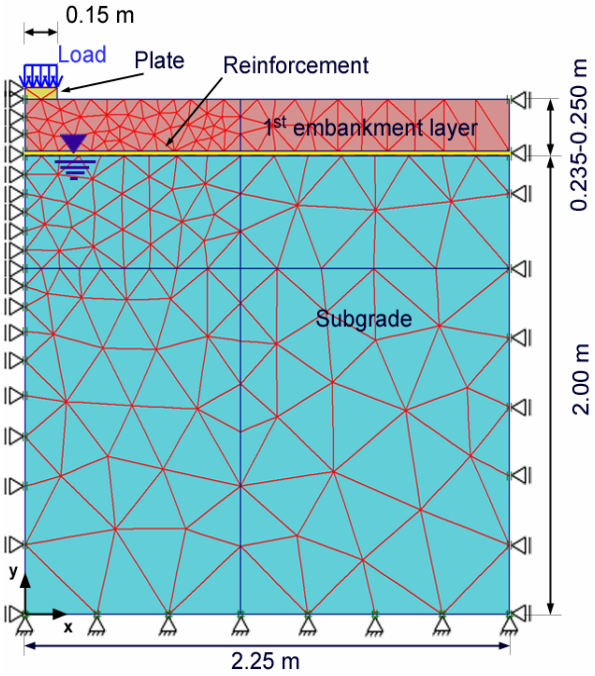

Figure 8 Axi-symmetric Finite Element discretization and boundary conditions

5.2 *Modelling of the construction processes*

During construction, the height of each layer (initial height of the loose material = ~ 25 cm) has been measured before and after compaction. These measurements have been used in the modelling to simulate the compaction. The measured settlements due to the compaction have been applied as a prescribed displacement on the surface of each embankment layer.

Table 4 Measurements of the layer thickness before/after compaction

Height [cm]	1st layer	2nd layer
Height before compaction	25.0	48.5
Height after compaction	23.5	45
Δ Height - prescribed displacement	1.5	3.5

The goal of this procedure was to take into account the hardening of the embankment layer due to the compaction. In combination with fixed horizontal borders it caused also an increase in horizontal stresses, a well-known effect of compaction (LANG et al., 2002). The same procedure has been applied for both layers, although no dynamic load has been used for the simulation of the dynamic compaction of the second layer as it would have exceeded the goal of this research. The time intervals between layer installations and tests were taken into account with a consolidation calculation.

The same load steps were applied to a plate lying on the centre line of the (axisymmetric) embankment layer to model the plate loading tests. The time between the loading steps being relatively short (~ 2 min.), undrained behaviour was considered for the subgrade.

Preliminary calculations showed that the soil-geogrid interfaces could cause instability in the calculation, when used in an updated mesh analysis. In some cases, a split has been observed between the soil-geogrid interface and the underlying soil cluster. Therefore the decision was taken not to use interfaces for the back-calculation. Instead of that, a thin soil layer was introduced between reinforcement and soil in the model with reduced shear strength pa-

rameter to simulate the interaction between soil and reinforcement.

5.3 *Constitutive models*

The subgrade was modelled using the Soft-Soil Model (SS) implemented in PLAXIS. This model allows plastic hardening (with associated flow) about the isotropic mean stress axis ($q = \sigma'_1-\sigma'_3 = 0$; $p' = \sigma'_1+\sigma'_2+\sigma'_3/3$) via a part of the standard Modified Cam Clay ellipse (on the "wet" side of a critical state line). This model is only suitable for soils with OCR between 1-1.5 because the softening behaviour at higher OCRs is not modelled. By using a cohesion value to represent peak states, it was possible to extend the wet side of the Soft-Soil model in terms of OCR and to make it more applicable for an OCR of 2.

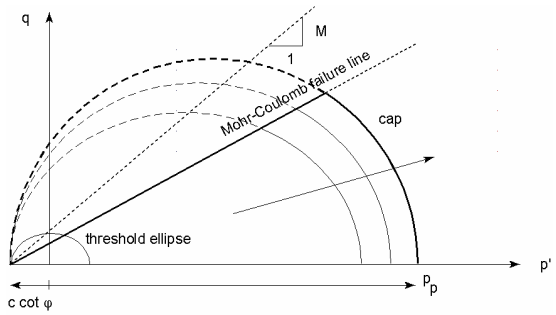

Figure 9 Yield surface of the Soft-Soil model in q-p'-plane. [BRINKGREVE, 2002]

The cap surfaces are intersected by a Mohr Coulomb failure line in the q – p'- diagram with defined according to an associated flow rule, since the dilation angle is zero. This line can not be moved or crossed and so a state of pure shear strain with zero volume change can not be reached at the critical state. In consequence, the soft soil model should only be used for normally consolidated soils for which yieldings occurs first via the cap.

The behaviour of the dense recycled material was modelled by using an available elasto-plastic constitutive model, called the Hardening-Soil model (HS). In this case, the model is a slightly extended version of the Soft-Soil model in which the elastoplasticity is allowing deviatoric hardening up to the Mohr-Coulomb condition. The constitutive models are further described in the literature (Brinkgreve, 2002).

The parameters of the embankment layers have been defined within a range with a parameter study and the influence of each has been investigated. The high reloading modulus (E_{ur}) of the second layer is possibly caused by crushing or abrasion of the recycled material during the first loading cycle resulting in a higher density. Due to the dynamic compaction of the second layer, a higher stiffness E_{oed} has been obtained. With this exception, the parameters of the second layer did correspond with those determined for the first layer.

Table 3 Soil parameters used in the Finite Element analysis

	1st/2nd Layer	Subgrade
γ_{dry} *[kN/m³]*	15	14.1
γ_{wet} *[kN/m³]*	18	18.1
Soil behaviour	drained	undrained
Soil Model	Hardening-Soil	Soft-Soil
c' *[kN/m²]*	7 *)	25
φ'	43° *)	14°
ψ'	11° *)	-
λ*	-	0.059
κ*	-	0.015
E_{50} [MN/m²]	20 *)	-
E_{oed} [MN/m²]	12.5(1st layer) *) 15 (2nd layer) *)	-
E_{ur} [MN/m²]	55 *)	-
m	0.5 *)	
Interaction-Soil-Geosyn.	0.9 **)	0.8 **)

*) assumed value **) reduced shear strength

6 COMPARISON FIELD TESTS VS FE-METHOD

The values given in Table 3 were adopted for the preliminary analyses, and the results for load-unload-reload cycles on both 1st and 2nd embankment layers are given in Figures 9 & 10. The results were in good accordance with the results of the field test. This has been confirmed as the second measured load-settlement curve could be calculated with the same parameters (with the exception of the higher E-Modulus of ΔE_{oed}= 2.5 MN/m²). Only the unload-reload-curves could not be back-calculated quite satisfactorily. This is due to the fact that the unloading and reloading stiffness are influenced by hysteresis but they are represented by only one equivalent modulus in both Hardening-Soil- and Soft-Soil-models.

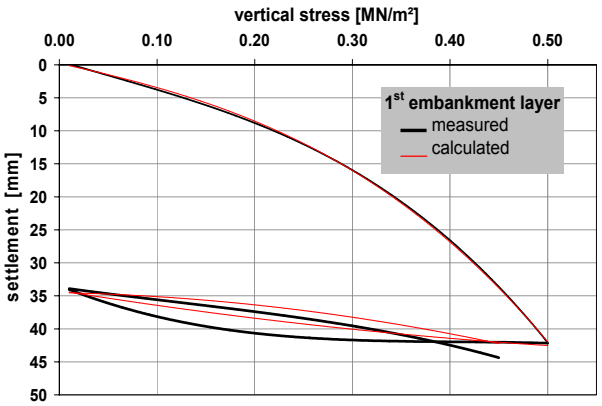

Figure 10 Calculated and measured load-settlement curves, 1st embankment layer

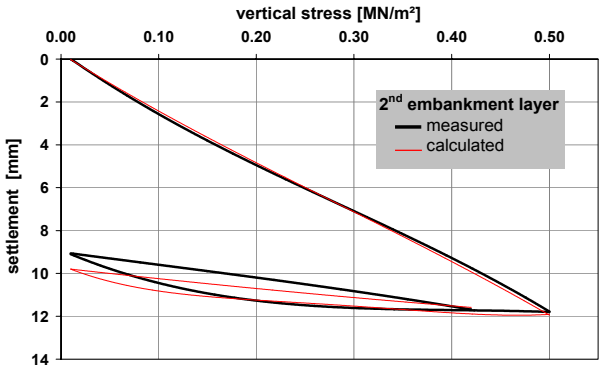

Figure 11 Calculated and measured load-settlement curves, 2nd embankment layer

The measured and the calculated strains in the geogrid (Figures 12 & 13) do not fit as well as the load-settlement curves shown above.

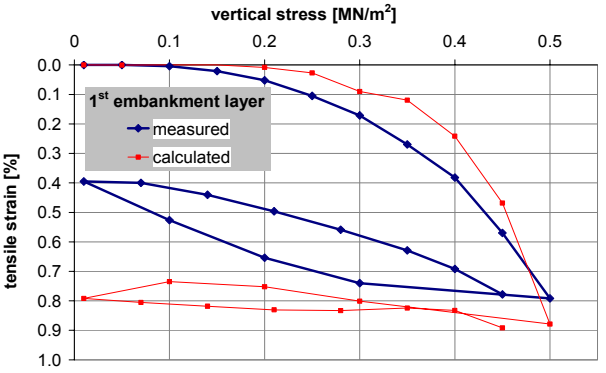

Figure 12 Calculated and measured load-tensile strain curves, strain gauge 2, 1st embankment layer, field 7, at a distance of 25 cm from the axis of the loading plate

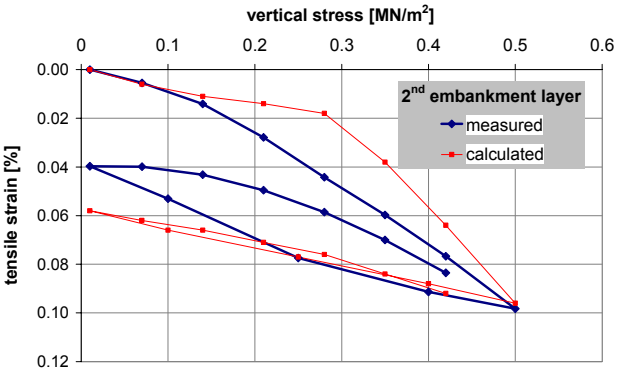

Figure 13 Measured and calculated load-tensile strain curves, DMS-2, 2nd embankment layer, field 7, at a distance of 25 cm from the axis of the loading plate

Many factors may have led to this discrepancy between measured and calculated strain. The plate loading tests had to be performed along the axis of the test track where no strain gauge was available. The nearest strain gauge was at a distance of about 25 cm on the direction perpendicular to the track axis and this has been considered in the calculations. But in an axi-symmetric system (also not in a plane strain system) it is not possible to simulate the case where the plate loading test and the strain gauge do not lie on the same line perpendicularly to the track. As an exact positioning of the test locations in the axis direction was very difficult to obtain, this could have led, at least partly, to the observed divergence.

Another possible factor for the discrepancy is that the geogrid may have been locally reinforced by the gluing of the strain gauges so that the tensile stiffness was higher in this zone.

7 FIRST APPLICATIONS

Following the back-analyses, various calculations with different geometry and parameters have been performed in order to analyse the reinforcement mechanism and the influence of the factors due to the modelling.

7.1 *Without reinforcement*

An interesting result is brought about by the calculation of an identical embankment model without a geogrid (Figure13). On the first embankment layer, a failure mechanism develops after the 7th loading step (350-400 kN/m²).

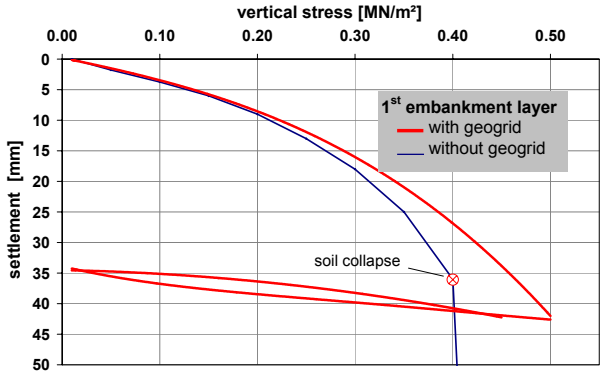

Figure 14 Calculated load-settlement curves, with/without geogrid, 1st embankment layer, field 7

Comparing the shear strains in the model with and without a geogrid in Figure 14, the well known reinforcement mechanism can be clearly observed. The shear stresses causing the deformations are taken over by the geogrid and the values of shear strain, as well as the extension of the shear zone, are significantly reduced.

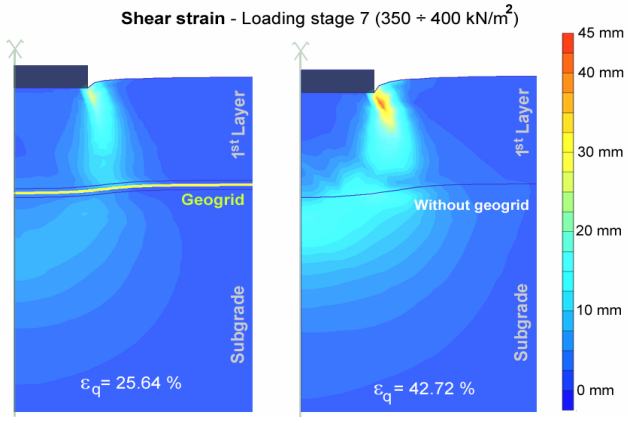

Figure 15 Comparison of calculated shear strain, with/without geogrid, 1st embankment layer, field 7

The comparison between the equivalent Young's moduli with and without a geogrid shows the increase in stiffness due to the geogrid, increase that could be even higher in the case of greater and wider loads (depth effect).

Table 5 Calculated Young's moduli E_1, E_2, with/without geogrid, 2nd embankment layer

Young's modulus [MN/m²]	E_1	E_2	E_2/E_1
With geogrid	9.61	51.42	4.18
Without geogrid	8.88	37.12	6.41
Differences	7.6 %	27.8 %	34.7%

The influence of the geogrid is less important for the second layer due to the greater layer thickness (Figure 16).

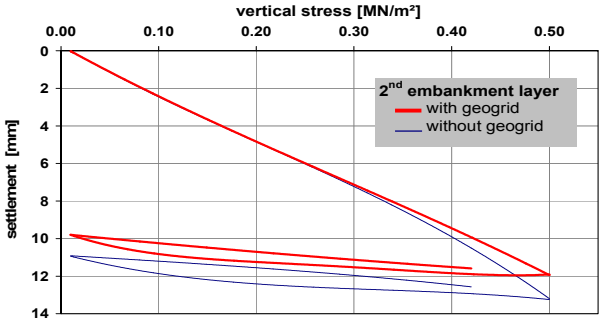

Figure 16 Calculated load-settlement curves, with/without geogrid, 2nd embankment layer, field 7

7.2 *Increasing the layer thickness*

In a next calculation without a geogrid, the thickness of the first layer has been increased until the end settlement under the first loading was equal to the end settlement of the model with geogrid and original thickness. This gives an idea of the quantity of embankment material that can be spared through the use of a geogrid. It can be seen from Figure 16 that in the case considered, a supplementary height of about 8 cm, i.e. 40 % of the original height, would have been necessary to reach the same end settlement.

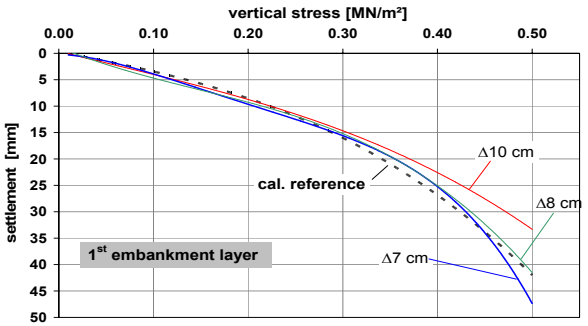

Figure 17 Calculated load-settlement curves, without geogrid and with higher embankment layer thickness, 1st embankment layer, field 7

8 CURRENT AND FUTURE RESEARCH

One of the main goals of the research project is to give guidelines for the analysis of the serviceability of geosynthetic reinforced construction with the help of numerical methods. In order to be able to give generally valid recommendations, a large number of methods and case studies must be analysed.

Further calculations are being performed to study the influence of the numerical methods (element forms, coarseness of the mesh, dimension of the mesh, iteration processes) in respect of other types of reinforced constructions.

It is also planned to do these calculations using different constitutive models for the soil and, if available, for the geosynthetics. The results should also be compared with those obtained with other software packages including 3D-Finite Element and also Finite Difference applications.

9 CONCLUSION

The results obtained in this study show that it is possible to model geosynthetic reinforced constructions with existing FE-programs by taking the construction process into account. However the calibration of the parameters is complex as the parameters required are dependent on the constitutive models available and this has to be considered during the modelling process. The different settings for the numerical modelling, such as discretization, iterations steps etc. also influence the results of the calculations.

The modelling of the plate loading test on a geosynthetic reinforced shallow embankment could be achieved with satisfying accuracy but the performed calculations still have some limitations. For example, simulating the compaction with the help of a prescribed displacement does not induce tensile stress in the geogrid as is caused by the compaction in the field.

The calculations made in this paper of the cases with and without geogrid do not reflect the reality completely. In fact the geogrid permits a higher compaction and prevents the subgrade from mixing with the embankment layer, so that a higher loading capacity is developed. This could not be modelled in the calculations, and in nature, the difference between the load-settlement curve with and without a geogrid would probably be even greater.

10 ACKNOWLEDGEMENTS

The authors thank the Swiss Federal Roads Authority for financial support and for permission to publish the results. BP Amoco Fabrics, Fritz Landolt AG, Tensar Int. GmbH, Huesker Synthetic GmbH, Sytec Bausysteme AG, Polyfelt Ges.m.b.H. and Naue Fasertechnik GmbH & Co KG kindly provided the geosynthetics and additional financial support. Many thanks are due to Sarah Springman for discussions about the constitutive modelling and for proofreading the manuscript. The contribution of Thomas Weber towards carrying the laboratory tests is also gratefully acknowledged.

11 REFERENCES

Brinkreve, R.B.J., 2002: PLAXIS 2D Version 8.2. Rotterdam: Balkema

Hufenus, R., Rüegger, R., Banjac, R., Mayor, P., Springman, S.M., Feltrin, G., Brönnimann, R., 2003: Verstärken von Fundationsschichten auf weichem Untergrund, Proceedings of the 8th Conf. on Synthetics in Geotechnics, Munich, pp. 171 – 179

Hufenus, R., 2003 Personal Communication

Hufenus, R., Rüegger, R., Weingart, K., Banjac, R., Mayor, P., Springman, S.M., Brönnimann, R., Feltrin, G., 2004: Reinforcing foundation layers on soft subgrade, EuroGeo3, Munich submitted paper

Lang, H.J., Huder, J., Amann, P., 2002: Bodenmechanik und Grundbau, Springer-Publisher, Zurich

Schanz, T., 1995: Untersuchungen zum mechanischem Verhalten granularer Gemische, Band 208, 7/95, IGT, Swiss Federal Institute of Technology Zurich

SN 670 317b, 1998: Soil; Plattendruckversuch E_V und M_E. - VSS, Zurich.